

# 1 The rhenium isotope composition of Atlantic Ocean seawater

2

3 Alexander J. Dickson<sup>1</sup>, Yu-Te Hsieh<sup>2</sup>, Allison Bryan<sup>2</sup>

4

5 1. Department of Earth Sciences, Royal Holloway University of London, Egham, Surrey, TW20  
6 0EX

7 2. Department of Earth Sciences, University of Oxford, South Parks Road, Oxford, OX1 3AN

8

## 9 **Abstract**

10 The concentrations and isotopic compositions of rhenium are presented from seawater samples  
11 obtained from the primary station for the Bermuda Atlantic Time Series Study in the North Atlantic  
12 Ocean and from the 40°S UK GEOTRACES expedition in the South Atlantic Ocean. Salinity-  
13 normalized Re concentrations in both locations range between ~6.8–7.7 ppt between 50–5000 m  
14 depth, consistent with previously published concentration data from the North Atlantic and North  
15 Pacific Oceans. Rhenium isotope values (expressed as  $\delta^{187/185}\text{Re}$  relative to NIST 3143) exhibit  
16 minimal variation around an average value of  $-0.17 \pm 0.12 \text{ ‰}$  ( $n = 12$ , 2 S.D.), irrespective of water  
17 depth or water mass. These results confirm that the isotopic composition of perrhenate ( $\text{ReO}_4^-$ ) in  
18 seawater is uniform. The new data establish a baseline for evaluating the isotopic mass balance of  
19 Re, and for future assessments of whether this global cycle can be disturbed by changes in seafloor  
20 redox and/or global weathering rates.

21

## 22 **Introduction**

23 The transition metal rhenium is useful for tracing the evolution of Earth's environmental systems over  
24 geological time. Rhenium is highly enriched over its typical continental crust concentration of 0.198  
25 pg/g in sedimentary deposits accumulating in reducing settings (Peucker-Ehrenbrink and Jahn,  
26 2001). These high sedimentary enrichments, which are typically the most pronounced of any redox-  
27 sensitive element (Brumsack, 2006), have been suggested to occur either due to the reduction of  
28 Re(VII) to Re(IV) (Colodner et al., 1993; Chappaz et al., 2008), the thiolation of Re(VII)-S species,  
29 or co-precipitation with Fe-Mo-S phases (Helz and Dolor, 2012; Vorlicek et al., 2012) near to the  
30 Fe(III)/Fe(II) redox couple (McKay et al., 1997; Morford et al., 2005, 2009).

31 Rhenium has two isotopes,  $^{187}\text{Re}$  and  $^{185}\text{Re}$ , which comprise ~63 % and 37 % of natural Re  
32 respectively (Gramlich et al., 1973). Net isotopic fractionation (mass dependent and nuclear volume)  
33 of up to 1.5 ‰ is predicted to occur between thiolated Re(VII)-S and reduced Re(IV) species, and  
34 the perrhenate ( $\text{ReO}_4^-$ ) that is the dominant species of Re in oxygenated seawater, with  $\text{ReO}_4^-$  having  
35 the highest isotopic composition (Miller et al., 2009, 2015). The removal of mass of Re with a lower  
36 isotopic composition than seawater into marine sediments accumulating in low-oxygen conditions  
37 would have the potential to alter the global seawater isotopic composition if these fluxes changed  
38 over geological time. This effect is the basis for the possible application of Re isotopes as a tracer

39 of global ocean redox, in a similar vein to molybdenum, uranium and thallium isotopes, among others  
40 (e.g. Stirling et al., 2008; Anderson et al., 2014; Owens et al., 2016; Kendall et al., 2017).

41 Conversely, the isotopic composition of Re in the oceans may also be perturbed by a change  
42 in the size or compositions of the input flux. The pre-anthropogenic global riverine Re concentration  
43 is  $\sim 11.2$  pmol/kg (Colodner et al., 1993; Miller et al., 2011), yielding an annual flux to the oceans of  
44  $\sim 4.3 \times 10^5$  mol/yr (Miller et al., 2011). This riverine flux is suggested to be largely controlled by the  
45 oxidation of organic carbon and sulfides from terrestrial rocks, as indicated by the close  
46 correspondence between dissolved Re and  $\text{SO}_4^{2-}$  concentrations in rivers globally (Miller et al.,  
47 2011), by the close correspondence between Re and organic carbon concentrations in oxidatively  
48 weathered soil and shale profiles (Peucker Ehrenbrink and Hannigan, 2000; Hilton et al., 2014), and  
49 by the high concentrations of Re associated with n-alkane insoluble organic compounds (Selby et  
50 al., 2007). Changes to the locus of Re weathering, from organic-rich to silicate rocks, could thus alter  
51 the size and compositions the Re flux to the oceans (Miller et al. 2015; Dellinger et al., 2020).

52 Unfortunately, the development of the Re isotope system as a proxy for either ocean redox  
53 or weathering is currently hindered by a lack of data on the various parts of the modern Re cycle:  
54 seawater, weathering fluxes, and sedimentary removal fluxes. This paper presents isotopic  
55 measurements of dissolved Re in seawater from two vertical profiles in the North and South Atlantic  
56 Oceans. These samples span a range of water masses sourced from distinct oceanic regions.  
57 Thermodynamic calculations predict that Re should exist in oxygenated seawater as the stable  
58 oxyanion perrhenate ( $\text{ReO}_4^-$ ) (Brookins, 1986). The concentration of Re in seawater has previously  
59 been determined to fall in the range  $\sim 7.29$ – $8.19$  pg/g ( $\sim 39$ – $44$  pM), with a relationship with salinity  
60 that confirms its generally conservative behaviour (Anbar et al., 1992; Colodner et al., 1993). The  
61 intention here is to characterize the isotopic signature of  $\text{ReO}_4^-$  in seawater; and to test whether this  
62 isotope signature is the same in different water masses. These data are an important first step to  
63 understanding the global isotopic mass balance of Re, and the processes that might cause this  
64 balance to change over geological timescales.

65

## 66 **Methods**

67 Samples were collected from the UK Geotraces 40°S expedition (GA10) and from the primary station  
68 of the Bermuda Atlantic Timeseries Study (BATS). Exact sample positions are noted in Fig. 1.  
69 Seawater samples were collected using either a stainless steel (BATS) or titanium (GEOTRACES)  
70 rosette, each equipped with 24 Ocean Test Equipment sampling bottles. Seawater was filtered on  
71 board into acid-cleaned HDPE containers using  $0.2 \mu\text{m}$  AcroPak™ polyethersulfone filters and  
72 acidified immediately with a small amount of distilled HCl to reach pH  $\sim 1.7$ .

73 For Re concentrations,  $\sim 20$  ml of filtered seawater was weighed directly into a Teflon vial and  
74 spiked with a  $^{185}\text{Re}$ -enriched spike solution. Vials were sealed and allowed to reflux for 24 hours to  
75 achieve spike-sample equilibrium. Subsequently they were evaporated to dryness, refluxed in a 3:1  
76 mixture of concentrated  $\text{HNO}_3$  and HCl, evaporated again to dryness and re-dissolved in 2 ml 0.2 M

77 HNO<sub>3</sub>. Re was purified from the seawater matrix using a small anion exchange column. The sample  
78 was loaded onto 200 µl clean, pre-conditioned AG1-X8 anion resin (200–400 mesh). Matrix elements  
79 were eluted using a further 2 ml 0.2 M HNO<sub>3</sub>, before Re was eluted with 2 ml 8M HNO<sub>3</sub>. Two different  
80 <sup>185</sup>Re spikes were used in the course of this study. For samples processed at the University of  
81 Oxford, the DTM (*Department of Terrestrial Magmatism, Washington, USA*) Re spike was used. For  
82 samples processed at Royal Holloway, a new spike solution was prepared from metal powder  
83 obtained from Oakridge National Laboratories. Full details of the spike calibration procedure and  
84 results are described in the supplementary information.

85 For Re isotopes, ~500 ml of water from each sample was evaporated dry in a class 10 laminar  
86 flow hood, and re-dissolved in 120 ml 0.25 M HCl. Procedural blanks were spiked with the RHUL  
87 <sup>185</sup>Re tracer and re-dissolved in the same volume of acid. Re was purified from matrix elements with  
88 a two-step column procedure. First, samples were loaded onto pre-cleaned 3 ml AG1-X8 (200–400  
89 mesh) anion exchange resin, with a further addition of 10 ml 0.25 M HCl to elute matrix elements.  
90 Thereafter, Re was eluted with 28 ml 8M HNO<sub>3</sub>. In the second step, each sample was evaporated  
91 to dryness, re-dissolved in 1 ml 1M HF/0.5M HCl and loaded onto 200 µl anion resin in Teflon  
92 columns. Matrix elements were eluted with further additions of 1ml 1M HF/0.5M HCl, 1 ml 4M HCl  
93 and 0.4 ml 3M HNO<sub>3</sub>. Re was eluted with 1.5 ml 8M HNO<sub>3</sub>. After each Re elution step, resin beads  
94 were visible in the Teflon sample vials. To minimize the effect of organic material on mass  
95 spectrometry, each sample was dissolved in a small volume of concentrated HNO<sub>3</sub> and ultra-pure  
96 H<sub>2</sub>O<sub>2</sub> and refluxed for 48 hours at 120°C. They were then evaporated dry and re-dissolved in 0.5 ml  
97 3% HNO<sub>3</sub>. The mass of Re recovered after columns was quantified during concentration check  
98 measurement runs by comparing a diluted aliquot of each sample to the signal intensities of external  
99 standards.

100 Re isotope ratios were measured in two laboratories. Several of the South Atlantic samples  
101 were measured at the University of Oxford using a Nu Instruments MC-ICP-MS attached to an ESI  
102 Apex sample introduction system with the spray chamber set to 100°C. This set up was required in  
103 order to achieve the requisite sensitivity in wet plasma mode to precisely monitor masses 185 and  
104 187. Samples were introduced as 10 ppb solutions to the instrument in 2% HNO<sub>3</sub>. Each  
105 measurement comprised a single block of 30x 10 s integrations, preceded by 10 integrations of blank  
106 2% HNO<sub>3</sub> to monitor backgrounds. Washout of Re to background levels between samples took ~ 5–  
107 10 minutes with 10% HNO<sub>3</sub> and 2% HNO<sub>3</sub>. Backgrounds rose throughout individual analysis  
108 sessions to as high as ~1.5% of the total analyte signal, but the measured composition of standards  
109 throughout the run did not notably change due to the background signal corrections.

110 Isotope ratios of the BATS samples and replicates of the South Atlantic samples were  
111 performed at Royal Holloway using a Neptune Plus MC-ICP-MS fitted with 10<sup>13</sup> Ω faraday resistors  
112 in wet plasma mode, with standard wet-plasma sample cones and 'H' skimmer cones. Samples were  
113 introduced to the instrument as 5 ppb solutions using a quartz SIS spray chamber. Each  
114 measurement comprised a single block of 40x 8.5 s integrations, preceded by 10 integrations of

115 blank 3% HNO<sub>3</sub>. Washout of Re to <0.1 % of the analyte signal was achieved using 3% HNO<sub>3</sub> in ~90  
116 s.

117 For both setups, instrumental mass bias was corrected by doping each sample to 30 or 40  
118 ppb W with NIST SRM 3163. This method offers a robust correction of the variable matrix  
119 contributions in each sample solution, given the similar ionization potentials of Re and W and their  
120 linearly related instrumental fractionation factors (Miller et al., 2009; Poirier and Doucelance, 2009;  
121 Dellinger et al., 2020). The W/Re ratios employed here (~6–8) were uniform between samples and  
122 bracketing standards, and thus do not affect the quality of isotope data via irregular formation of  
123 hydrides or peak tailing/abundance sensitivity effects (Dellinger et al., 2020). Measured ratios were  
124 corrected for instrumental bias by normalizing to a <sup>186</sup>W/<sup>184</sup>W ratio of 0.92767 and applying this to  
125 the measured <sup>187</sup>Re/<sup>185</sup>Re ratios using an exponential mass bias law (Miller et al., 2009).  $\delta^{187/185}\text{Re}$   
126 values were then calculated relative to bracketing measurements of NIST SRM 3143:  $\delta^{187/185}\text{Re} =$   
127  $[(^{187}\text{Re}/^{185}\text{Re}_{\text{sample}} - ^{187}\text{Re}/^{185}\text{Re}_{\text{NIST}}) / ^{187}\text{Re}/^{185}\text{Re}_{\text{NIST}}] * 1000$ . The potential interference of <sup>187</sup>O<sub>s</sub> on  
128 <sup>187</sup>Re was corrected by simultaneously monitoring <sup>189</sup>O<sub>s</sub> during each static measurement. Inter-  
129 laboratory accuracy of Re isotope data was monitored through the use of several secondary solution  
130 standards: an ICP Re concentration standard, a solution of H Cross company high purity Re wire,  
131 NIST SRM 989 and DURH-Re 1. Rhenium isotope ratios of spiked seawater concentration samples  
132 were determined from ~250 pg/g solutions by an identical measurement procedure as for isotope  
133 ratios, and calculated by isotope dilution from mass-bias corrected <sup>185</sup>Re/<sup>187</sup>Re ratios.

134

## 135 **Results**

136 The isotopic compositions of Re standard solutions are presented in Table 1 and seawater Re  
137 concentration and isotopic data are presented in Table 2. Seawater concentrations average 7.23  
138 pg/g across the entire dataset. Re isotope compositions are uniform within their uncertainties and  
139 average  $-0.17 \pm 0.12$  ‰.

140

## 141 **Discussion**

### 142 *Data quality and inter-laboratory accuracy*

143 The external reproducibility of Re solution standards improves to  $<\pm 0.1$  ‰ at analyte concentrations  
144  $>2$  ppb, while internal 2 S.E. counting uncertainties improve to  $<\pm 0.06$  ‰ at signal intensities of  $>\sim 50$   
145 mV for <sup>187</sup>Re (Fig. S2). The low uncertainties at low sample voltages are due to the use of  $10^{13}$  Ω  
146 Faraday resistors that increase the signal/noise ratio of small Re beams. For typical measurement  
147 concentrations of 4–5 ppb Re, internal errors are approximately  $\pm 0.07$  ‰, which are comparable to  
148 the results of Dellinger et al. (2020) for similar size sample beams using an identical analytical setup.

149 Measurements of secondary solution standards indicate excellent inter-laboratory accuracy  
150 (Table 1). The mean  $\delta^{187/185}\text{Re}$  determined here of NIST SRM 989 relative to NIST SRM 3143, for  
151 analyte concentrations  $>4$  ppb, was  $-0.26 \pm 0.1$  ‰, which is within uncertainty of the value determined  
152 by Miller et al. (2009) of  $-0.29 \pm 0.07$  ‰ and the value determined by Dellinger et al. (2020) of  $-0.28$

153  $\pm 0.04$  ‰. Similarly, a solution of high-purity Re wire obtained from H Cross company by Miller et al.  
154 (2009) yielded a  $\delta^{187/185}\text{Re}$  of  $-0.01 \pm 0.12$  ‰ (re-normalized to NIST 3143); a different aliquot of H  
155 Cross Re wire prepared during this study yielded a composition of  $-0.02 \pm 0.1$  ‰. Inter-laboratory  
156 accuracy is further demonstrated by the similarity in the composition of the DURH-1 Re standard  
157 characterized by Dellinger et al. (2020) as  $0.16 \pm 0.03$  ‰, (relative to NIST 3143) and at Royal  
158 Holloway in this study ( $0.13 \pm 0.04$  ‰). Finally, the mean  $\delta^{187/185}\text{Re}$  values of an in-house ICP Re  
159 solution standard analysed at Royal Holloway and Oxford during the course of this study were the  
160 same within uncertainties, suggesting that the data produced in both labs is comparable.

161 Procedural blanks, as determined by isotope dilution for concentration and stable isotope  
162 measurements, were 4–8 pg, constituting a tiny amount of the total Re processed. Concentration  
163 measurements were blank corrected, while isotope measurements were not. Miller et al. (2009), Liu  
164 (2015) and Dellinger et al. (2020) showed that ~60% of Re need to be eluted from AG1-X8 resin  
165 with 4M  $\text{HNO}_3$  to minimize column fractionation to within an uncertainty of  $\pm 0.1$  ‰ from the ‘true’  
166 value. Re recoveries in this study were between ~63% and ~100% (Table 2), which are large enough  
167 to avoid measurable fractionation. In any case, we used 7.5 M  $\text{HNO}_3$  to elute Re: Dellinger et al.  
168 (2020) showed that column fractionation effects are negligible when eluting Re with 8M  $\text{HNO}_3$ .

169

#### 170 *Atlantic seawater Re concentration data*

171 The blank-corrected and salinity-normalized concentrations of the BATS seawater samples  
172 measured at RHUL range from 6.79–7.42 pg/g, with an average of 7.16 pg/g. These concentrations  
173 are similar to those from the South Atlantic measured in the same lab, which range from 6.86–7.42  
174 pg/g (average 7.11 pg/g). The South Atlantic samples measured in Oxford using the DTM  $^{185}\text{Re}$   
175 spike have systematically higher concentrations (7.51–7.81 pg/g, average 7.58 pg/g) that are  
176 probably due to the precision of the calibrated concentrations of the DTM and RHUL  $^{185}\text{Re}$  spike  
177 solutions. Two samples (BATS 50 m and BATS 2000 m) were measured at RHUL using four  
178 separately spiked aliquots of seawater to assess external reproducibility, accounting for the full  
179 chemical separation and measurement procedure. These replicates indicate a precision of ~4–7%  
180 on the calculated concentrations. The apparent difference in the seawater concentrations measured  
181 on the same samples at RHUL and Oxford is therefore not resolvable outside of the uncertainties.

182 The average concentration of all BATS samples is  $7.16 \pm 0.34$  pg/g (2 S.D.), and the average  
183 of the South Atlantic samples is  $7.58 \pm 0.25$  pg/g. The variability in the entire dataset (~5%) is close  
184 to that of the sample replicates, thus suggesting that most of the inter-sample variation is related to  
185 procedural uncertainties (determination of  $^{185}\text{Re}/^{187}\text{Re}$  ratios, procedural blanks, spike-sample  
186 equilibration) rather than variation within the water column. Concentrations are therefore invariant  
187 with depth (Fig. 1). The mean Re concentrations determined in this study are close to the mean  
188 concentration of  $7.42 \pm 0.04$  pg/g for North Pacific seawater measured by Anbar et al. (1992) and  
189 thus confirm the homogeneity of seawater Re concentrations in different ocean basins.

190

191 *Atlantic seawater  $\delta^{187/185}\text{Re}$  compositions*

192 The isotopic compositions of seawater determined for the BATS samples range from  $-0.07 \pm 0.06$   
193 ‰ to  $-0.23 \pm 0.06$  ‰, and average  $-0.18$  ‰. Excluding one anomalously low replicate ( $> 2$  S.D.  
194 deviance from the whole dataset), the average is  $-0.20$  ‰. The Re isotope compositions of the South  
195 Atlantic samples range from  $-0.08 \pm 0.06$  ‰ to  $-0.21 \pm 0.06$  ‰ and average  $-0.14$  ‰. As for the Re  
196 concentration data, the BATS and South Atlantic isotope data are therefore not distinguishable  
197 outside of the external reproducibility of the method ( $\pm 0.07$  ‰) and are uniform with depth. The data  
198 provide constraints on the isotopic composition of several major water masses (North Atlantic Deep  
199 Water, Circumpolar Deep Water, Antarctic Intermediate Water, Weddell Sea Deep Water) which  
200 exhibit significant differences in water mass chemistry based on traditional nutrient tracers (e.g.  
201 phosphate concentrations, Fig. 1) but lack any resolvable differences in  $\delta^{187/185}\text{Re}$ . The lack of depth-  
202 dependency in the data is consistent with evidence that Re is not involved in biological processes  
203 and therefore not prone to re-mobilisation within the water column during organic matter production  
204 and subsequent oxidation (Pilato and Steifel, 1999).

205 The Atlantic seawater Re-isotope composition determined here can be considered  
206 representative of the stable perrhenate ion  $\text{ReO}_4^-$  that constitutes the vast majority of Re in the  
207 oceans under typical Eh-pH conditions (Brookins, 1986; Anbar et al., 1992; Colodner et al., 1993;  
208 Koide et al., 1995). The close agreement between the  $\delta^{187/185}\text{Re}$  data from natural samples and the  
209  $\delta^{187/185}\text{Re}$  composition of the IAPSO seawater standard measured by Dellinger et al. (2020) supports  
210 this argument. Additional studies of  $\delta^{187/185}\text{Re}$  in ocean seawater may yet reveal isotopic differences  
211 related to the thiolation, reduction, or sorption of Re under low oxygen or ferruginous conditions, as  
212 identified for other dissolved trace metals such as Cd (Janssen et al., 2014; Guinoiseau et al., 2018).  
213 *Ab initio* calculations of  $\delta^{187/185}\text{Re}$  for thiolated and reduced Re species suggest that where such  
214 effects are found, they would be liable to produce reaction products with isotopic compositions lower  
215 than  $\text{ReO}_4^-$  (Miller et al., 2015). Nonetheless, it is unclear if such effects would be detectable in the  
216 open ocean given the need for reaction products to be removed from seawater on timescales faster  
217 than localized ocean mixing. Such effects might be detectable in marginal marine basins where  
218 water renewal rates are low, or in stably low oxygen open ocean environments, perhaps above the  
219 sediment water interface of upwelling zones.

220

221 *Isotopic mass balance of Re*

222 Determining the  $\delta^{187/185}\text{Re}$  composition of oceanic  $\text{ReO}_4^-$  provides a starting point for evaluating the  
223 isotopic mass balance of Re in the modern ocean. This task is vital as a first step towards  
224 understanding what processes might have perturbed the isotopic system in the geological past.  
225 Since *ab-initio* calculations of thiolated and reduced Re species (those likely to be buried in marine  
226 sediments) are all isotopically lower than  $\text{ReO}_4^-$  (Miller et al., 2015), the likely isotopic composition of  
227 crustal weathering must also be  $\leq -0.17$  ‰ for the Re cycle to achieve steady-state. Figure 2 shows  
228 predicted compositions of Re weathering fluxes for Re removal into sediments for different

229 proportions of  $\text{Re(VII)O}_3\text{S}^-$  (with a composition 0.33 ‰ lower than seawater),  $\text{Re(IV)Cl}_6^{2-}$  (with a  
230 composition 1.52 ‰ lower than seawater) and ‘quantitative’ Re removal, with no isotopic  
231 fractionation from seawater (as observed in the modern ocean for Mo and Zn in euxinic settings).  
232 These calculations all indicate an input flux composition that is isotopically lower than seawater, but  
233 which could theoretically range anywhere from  $\sim -0.20$  ‰ to  $\sim -1.7$  ‰.

234 A large proportion of the Re weathered into the oceans is probably sourced from the oxidation  
235 of organic matter in sedimentary rocks (Peucker Ehrenbrink and Hannigan, 2000; Hilton et al., 2014).  
236 Miller et al. (2015) measured the isotopic composition of Re in samples from a Devonian Shale  
237 weathering profile and found that unweathered organic-rich shale had a value of  $-0.57$  ‰  
238 (renormalized to NIST 3143). Furthermore, basalt standards analysed by Dellinger et al. (2020)  
239 average  $\sim -0.33$  ‰. Both of these studies are consistent with the prediction in Fig. 2 that weathering  
240 inputs must have  $\delta^{187/185}\text{Re}$  compositions lower than seawater ( $-0.17$  ‰), but neither they nor the  
241 new seawater data can be used to make more precise constraints on this composition. It should also  
242 be considered that while  $\text{Re(VII)-S}$  and  $\text{Re(IV)}$  species are predicted to have lower  $\delta^{187/185}\text{Re}$   
243 compositions than seawater  $\text{ReO}_4^-$ , the potential for Re to be removed from seawater with a heavy  
244 isotopic composition, perhaps by adsorption to organic matter or mineral surfaces, cannot be  
245 presently excluded. Lastly, as with all isotope systems, construction of a modern isotopic mass  
246 balance for Re proceeds on the assumption that the system is in steady state. However, given the  
247 potential for rapid changes in Re weathering and burial over timescales of  $10^3$  years (e.g. Crusius et  
248 al., 1996; Hilton et al., 2014), this condition may not be met in the modern ocean.

249 A significant amount of work is therefore required to establish more precise constraints on  
250 the compositions of input and output fluxes of Re to and from the oceans, to allow an improved  
251 understanding of how this isotopic system may be utilized to reconstruct oceanic redox and/or  
252 weathering processes in the geological past.

253

## 254 **Conclusions**

255 Re concentration and  $\delta^{187/185}\text{Re}$  data are presented from the BATS primary sampling site in the North  
256 Atlantic Ocean and from the GEOTRACES 40°S (GA10) transect in the South Atlantic Ocean.  
257 Vertical differences in Re concentrations are not discernable outside of analytical uncertainties and  
258 are close to previous estimates of Re concentrations in Pacific seawater. The  $\delta^{187/185}\text{Re}$  of the  
259 samples average  $\sim -0.17 \pm 0.12$  ‰ and are invariant vertically and with latitude. This value therefore  
260 characterizes the  $\text{Re(VII)O}_4^-$  that constitutes the majority of dissolved Re in the oceans and provides  
261 a starting point for evaluating the isotopic mass balance of Re. If sedimentary output fluxes of Re  
262 are assumed to have  $\delta^{187/185}\text{Re}$  compositions lower than seawater (Miller et al., 2015), the  
263 weathering input flux of Re to the oceans can be predicted to also be  $< -0.20$  ‰. Although a small  
264 number of constraints exist on the composition of weathered Re (Miller et al., 2015; Dellinger et al.,  
265 2020), more precise estimates of this parameter must await future measurements of Re in rivers,  
266 marine sediments and continental crust rocks. A final, important point is that given the unavailability

267 of Re isotopic standard NIST SRM 989, we suggest that future studies of Re isotopes should use  
268 NIST SRM 3143 as a zero-delta reference. The isotopic composition of this solution relative to NIST  
269 989 has now been determined in three different laboratories as +0.29 ‰ (Table 1), and therefore  
270 future studies using NIST 3143 will be directly comparable to the pioneering efforts of Miller et al.  
271 (2009, 2015) and Dellinger et al. (2020).

272

### 273 **Acknowledgements**

274 We thank Mathieu Dellinger and Bob Hilton for kindly sharing aliquots of NIST 989 and the DUR-Re-  
275 1 solution standards. We also thank Anthony Chappaz for many fruitful discussions on Re isotopes  
276 during the course of this study. AJD acknowledges a Royal Holloway Research Strategy Fund award  
277 that supported this work.

278

### 279 **References**

280 Anbar, A.D., Creaser, R.A., Papanastassiou, D.A. and Wasserburg, G.J. (1992), Rhenium in  
281 seawater: confirmation of generally conservative behavior. *Geochimica et Cosmochimica Acta* 56,  
282 4099–4103.

283

284 Anderson, M.B., Romaniello, S., Vance, D., Little, S.H., Herdman, R. and Lyons, T.W. (2014), A  
285 modern framework for the interpretation of  $^{238}\text{U}/^{235}\text{U}$  in studies of ancient ocean redox. *Earth and*  
286 *Planetary Science Letters* 400, 184–194.

287

288 Brookins, D.G. (1986), Rhenium as analog for fissigenic technetium: Eh-pH diagram (25°C, 1 bar)  
289 constraints. *Applied Geochemistry* A, 513–517.

290

291 Brumsack, H-J. (2006), The trace metal content of recent organic carbon-rich sediments:  
292 implications for Cretaceous black shale formation. *Palaeogeography, Palaeoclimatology,*  
293 *Palaeoecology* 232, 344–361.

294

295 Chappaz, A., Gobeil, C. and Tessier, A. (2008), Sequestration mechanisms and anthropogenic  
296 inputs of rhenium in sediments from eastern Canada lakes. *Geochimica et Cosmochimica Acta* 72,  
297 6027–6036.

298

299 Colodner, D., Sachs, J., Ravizza, G., Turekian, K., Edmond, J. and Boyle, E. (1993), The  
300 geochemical cycle of rhenium: a reconnaissance. *Earth and Planetary Science Letters* 117, 205–  
301 221.

302

303 Crusius, J., Calvert, S., Pedersen, T. and Sage, D. (1996), Rhenium and molybdenum enrichments  
304 in sediments as indicators of oxic, suboxic and sulfidic conditions of deposition. *Earth and Planetary*  
305 *Sciences Letters* 145, 65–78.

306

307 Dellinger, M. Hilton, R.G. and Nowell, G.M. (2020), Measurements of rhenium isotopic composition  
308 in low-abundance samples. *Journal of Analytical Atomic Spectrometry*, DOI:10.1039/c9ja00288j.

309

310 Gramlich, J.W., Murphy, T.J., Garner, E.L. and Shields, W.R. (1973), Absolute isotopic abundance  
311 ratio and atomic weight of a reference sample of rhenium. *Journal of Research of the National*  
312 *Bureau of Standards* 77A, 691–698.

313

314 Guinoiseau, D., Galer, S.J.G. and Abouchami, W. (2018), Effect of cadmium sulfide precipitation on  
315 the partitioning of Cd isotopes: implications for the oceanic Cd cycle. *Earth and Planetary Science*  
316 *Letters* 498, 300–308.

317  
318 Helz, G.R. and Dolor, M.K. (2012), What regulates rhenium deposition in euxinic basins? *Chemical*  
319 *Geology* 304–305, 131–141.  
320  
321 Hilton, R.G., Gaillardet, J., Calmels, D. and Birck, J-L. (2014), Geological respiration of a mountain  
322 belt revealed by the trace element rhenium. *Earth and Planetary Science Letters* 403, 27–36.  
323  
324 Janssen, D.L., Conway, T.M., John, S.G., Christian, J.R., Kramer, D.I., Pedersen, T.F. and Cullen,  
325 J.T. (2014), Undocumented water column sink for cadmium in open ocean oxygen-deficient zones.  
326 *Proceedings of the National Academy of Sciences USA* 111, 6888–6893.  
327  
328 Liu, R. (2015), Rhenium isotopic compositions of iron meteorites. MSc Thesis, Florida State  
329 University.  
330  
331 McKay, J.J., Pedersen, T.F. and Mucci, A. (2007), Sedimentary redox conditions in continental  
332 margin sediments (NE Pacific)- influence on the accumulation of redox-sensitive trace metals.  
333 *Chemical Geology* 238, 180–196.  
334  
335 Kendall, B., Dahl, T.W. and Anbar, A.D. (2017), The stable isotope geochemistry of molybdenum.  
336 *Reviews in Mineralogy and Geochemistry* 82, 683–732.  
337  
338 Koide, M., Hodge, V.F., Yany, J., Stallard, M., Goldberg, E., Calhoun, J. and Bertine, K. (1986),  
339 Some comparative marine geochemistries of rhenium, gold, silver and molybdenum. *Applied*  
340 *Geochemistry* 1, 705–714.  
341  
342 Miller, C.A., Peucker-Ehrenbrink, B. and Ball, L. (2009), Precise determination of rhenium isotope  
343 composition by multi-collector inductively-coupled plasma mass spectrometry. *Journal of Analytical*  
344 *Atomic Spectrometry* 24, 1069–1078.  
345  
346 Miller, C.A., Peucker-Ehrenbrink, B. and Schauble, E.A. (2015), Theoretical modeling of rhenium  
347 isotope fractionation, natural variations across a black shale weathering profile, and potential as a  
348 paleoredox proxy. *Earth and Planetary Science Letters* 430, 339–348.  
349  
350 Morford, J.L., Emerson, S.R., Breckel, E.J. and Kim, S.H. (2005), Diagenesis of oxyanions (V, U, Re  
351 and Mo) in pore waters and sediments from a continental margin. *Geochimica et Cosmochimica*  
352 *Acta* 69, 5021–5032.  
353  
354 Morford, J.L., Martin, W.R., François, R. and Carney, C.M. (2009), A model for uranium, rhenium  
355 and molybdenum diagenesis in marine sediments based on results from coastal locations.  
356 *Geochimica et Cosmochimica Acta* 73, 2938–2960.  
357  
358 Owens, J.D., Nielsen, S.G., Horner, T.J., Ostrander, C.M. and Peterson, L. (2017), Thallium isotopic  
359 compositions of euxinic sediments as a proxy for global manganese oxide burial. *Geochimica et*  
360 *Cosmochimica Acta* 213, 291–307.  
361  
362 Peucker-Ehrenbrink, B. and Hannigan, R.E. (2000), Effects of black shale weathering on the mobility  
363 of rhenium and platinum group elements. *Geology* 28, 475–478.  
364  
365 Peucker-Ehrenbrink, B. and Jahn, B.M. (2001), Rhenium-osmium isotope systematics and platinum-  
366 group elements concentrations: loess and the upper continental crust. *Geochemistry Geophysics*  
367 *Geosystems* 2, 1061, doi:10.1029/2001GC000172.  
368  
369 Pilato, R.S. and Stiefel, E.I. (1999), Molybdenum and tungsten enzymes. In Reedijk, J. and  
370 Bouwman, E. (eds.), *Bioinorganic catalysis* 2, 81–152. Marcel Dekker, New York.  
371

372 Poirier, A and Doucelance, R. (2009), Effective correction of mass bias for rhenium measurements  
373 using MC-ICP-MS. *Geostandards and Geoanalytical Research* 33, doi:10.1111/j.1751-  
374 908X.2009.00017.x  
375  
376 Selby, D., Creaser, R.A. and Fowler, M.G. (2007), Re-Os elemental and isotope systematics in crude  
377 oils. *Geochimica et Cosmochimica Acta* 71, 378–386.  
378  
379 Sheen, A.I., Kendall, B., Reinhard, C.T., Creaser, R.A., Lyons, T.W., Bekker, A., Poulton, S.W. and  
380 Anbar, A.D. (2018), A model for the oceanic mass balance of rhenium and implications for the extent  
381 of Proterozoic ocean anoxia. *Geochimica et Cosmochimica Acta* 227, 75–95.  
382  
383 Stirling, C.H., Andersen, M.B., Potter, E-K. and Halliday, A.N. (2007), Low-temperature isotopic  
384 fractionation of uranium. *Earth and Planetary Science Letters* 264, 208–225.  
385  
386 Vorlicek, T., Chappaz, A., Groskreutz, L.M., Young, N., Lyons, T.W. (2015), A new analytical  
387 approach to determining Mo and Re speciation in sulfidic waters. *Chemical Geology* 403, 52–57.  
388  
389  
390

## 391 **Figures**

392 **Figure 1:** Re concentrations and isotope compositions for (A) the North Atlantic BATS primary site  
393 and (B) for the GEOTRACES GA10 40°S transect. The plots to the left of each panel show sample  
394 positions superimposed onto water mass dissolved phosphate concentrations extracted from the  
395 World Ocean Atlas 2009. Phosphate concentrations are in units of  $\mu\text{M}$ . Primary water masses are  
396 also displayed. Vertical dashed lines indicate the mean isotopic composition and concentration of all  
397 seawater samples analysed. NADW: North Atlantic Deep Water. AABW: Antarctic Bottom Water.  
398 SACW: South Atlantic Central Water. SAMW: Sub-Antarctic mode Water. AAIW: Antarctic  
399 Intermediate Water. WSDW: Weddell Sea Deep Water.

400  
401 **Figure 2:** Mass balance model showing the predicted  $\delta^{187/185}\text{Re}$  composition of Re weathered into  
402 the ocean. The calculated weathering compositions (dashed lines) assume a steady-state system  
403 and different fractional combinations of sedimentary output fluxes of Re as (i)  $\text{Re(IV)Cl}_6^{2-}$  and  
404  $\text{Re(VII)O}_3\text{S}^-$ ; and (ii)  $\text{Re(IV)Cl}_6^{2-}$  and ‘quantitative’ removal of Re into sediments. These removal  
405 species/mechanisms were chosen because they cover the largest isotopic range predicted by *ab*  
406 *initio* calculations (Miller et al., 2015), thus yielding the largest possible range of compositions for the  
407 input fluxes. Arrows indicate the composition of unweathered shales and basalt standards measured  
408 by Miller et al. (2015) and Dellinger et al. (2020) respectively.

## 410 **Tables**

411 **Table 1:** Compilation of standard solutions analysed in this study, Miller et al. (2009) and Dellinger  
412 et al. (2020). All  $\delta^{187/185}\text{Re}$  compositions are referenced to NIST 3143 as the zero delta. Uncertainties  
413 are the external reproducibilities calculated from several measurements of each solution and are  
414 typically slightly larger than the measured internal errors.

415

Standard	Average $\pm$ 2 S.D. (‰ rel. to NIST 3143), RHUL	Average $\pm$ 2 S.D. (‰ rel. to NIST 3143), OXFORD	Miller et al., Average $\pm$ 2 S.D. (‰ rel. to NIST 3143), WHOI	Dellinger et al., Average $\pm$ 2 S.D. (‰ rel. to NIST 3143), DURHAM
NIST 3143	0 $\pm$ 0.08	0 $\pm$ 0.08	0	-
NIST 989	-0.27 $\pm$ 0.10 (n = 14)	-	-0.29 $\pm$ 0.07	-0.28 $\pm$ 0.04
ICP Re	-0.15 $\pm$ 0.07 (n = 21)	-0.19 $\pm$ 0.09 (n = 13)	-	-
H Cross Re wire	-0.02 $\pm$ 0.10 (n = 9)	-	-0.01 $\pm$ 0.12	-
DURH-Re 1	0.14 $\pm$ 0.03 (n = 3)	-	-	0.16 $\pm$ 0.03

416

417

418

**Table 2:** BATS data.

Sample	Salinity (PSU)	Re concentration (pg/g)	$\delta^{187/185}\text{Re}$ (‰ NIST 3143)	2 S.E.	% Recovery
50 m	36.61	7.01			
50 m	36.61	7.36			
50 m	36.61	6.79			
50 m	36.61	6.94			
200 m	36.58	7.40	-0.22	0.10	63
200 m	36.58	6.86			
400 m	36.50	7.18	-0.23	0.06	82
800 m	35.29	7.11	-0.21	0.06	108
800 m	35.29	7.20			
1000 m	35.09	7.10	-0.19	0.06	107
1000 m	35.09	7.06			
2000 m	34.97	7.31			
2000 m	34.97	7.03			
2000 m	34.97	7.42			
2000 m	34.97	7.11			
3000 m	34.92	7.27	-0.25	0.09	85
3000 m	34.92	7.38	-0.07	0.06	72
4500 m	34.88	7.13	-0.21	0.06	88
4500 m	34.88	7.41			

419

420

421

422

423

**Table 3:** 40°S GEOTRACES GA10 data. Samples marked with an asterisk are from Oxford. All other samples were analysed at RHUL.

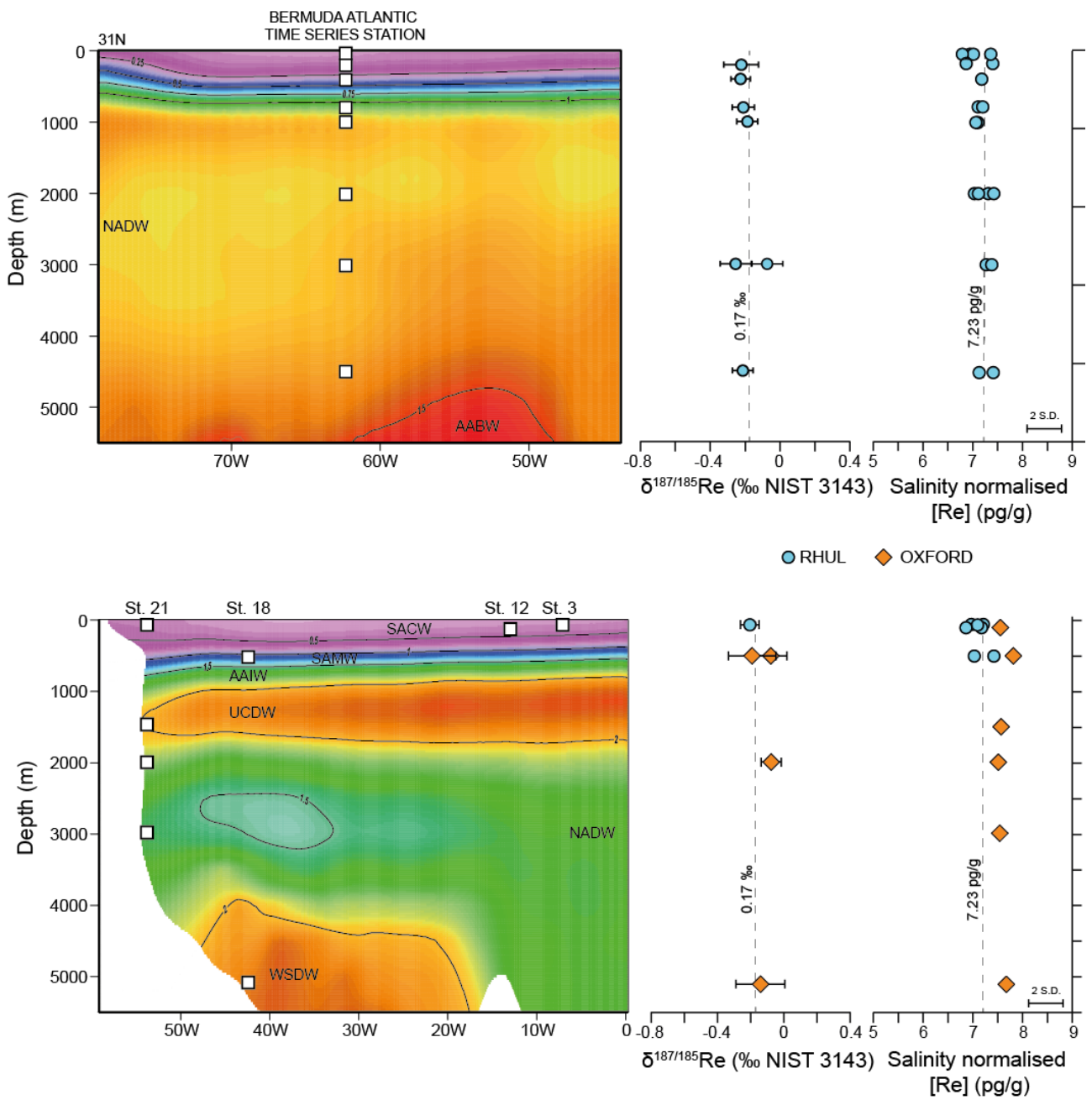
GEOTRACES Bottle code	Water depth (m)	Salinity (PSU)	Re concentration (pg/g)	$\delta^{187/185}\text{Re}$ (‰ NIST 3143)	2 S.E.	% Recovery
0179	51	34.88	6.96			
0179	51	34.88	7.21			
2327	58	36.72	7.09	-0.21	0.06	98
1550	97	35.26	6.86			
1550	97	35.26	7.17			
1550*	97	35.26	7.55			
2006	496	34.18	7.02			
2006	496	34.18	7.42			
2006*	496	34.18	7.81	-0.19	0.14	70
2006*	496	34.18		-0.08	0.10	72
2279*	1492	34.47	7.56			
2276*	1988	34.80	7.51	-0.08	0.06	76
2269*	2985	34.75	7.54			
1952*	5103	34.67	7.67	-0.14	0.15	81

424

425

426  
427  
428  
429  
430  
431  
432  
433  
434  
435

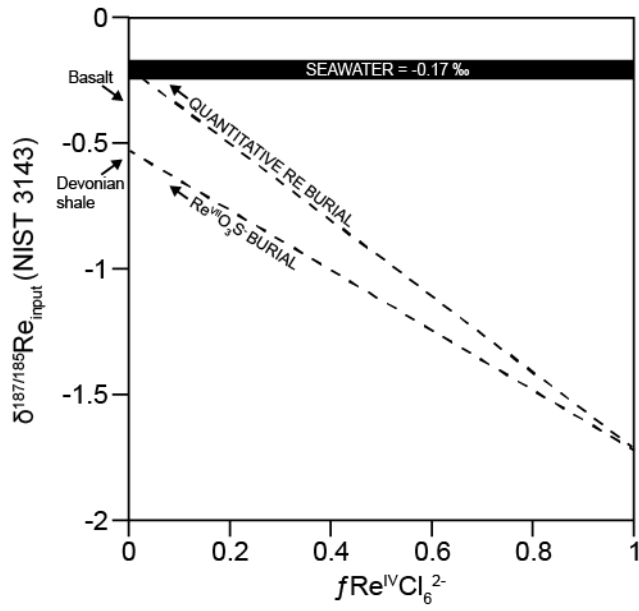
Figure 1



436  
437  
438

439  
440  
441  
442  
443  
444  
445  
446

Figure 2



447  
448  
449  
450  
451